



Cite this: DOI: 10.1039/c5cc02502h

Received 26th March 2015,  
Accepted 12th May 2015

DOI: 10.1039/c5cc02502h

www.rsc.org/chemcomm

# A new redox strategy for low-temperature formation of strong basicity on mesoporous silica†

Li Zhu, Feng Lu, Xiao-Dan Liu, Xiao-Qin Liu and Lin-Bing Sun\*

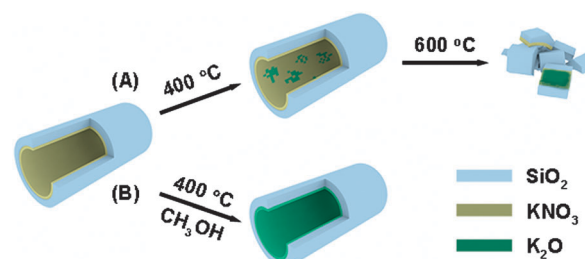
**A redox strategy was designed to generate strong basicity on mesoporous silica by using the redox interaction of a precursor with methanol vapor. The formation of strongly basic sites was realized at 400 °C, which breaks the tradition of thermally induced decomposition that usually requires much higher temperatures (> 600 °C).**

For the demands of sustainable development and green chemistry, increasing attention has been paid to the replacement of conventional homogeneous catalytic processes with heterogeneous ones.<sup>1</sup> Among various heterogeneous catalysts, mesoporous solid strong bases are of great interest due to some remarkable advantages such as no corrosion, facile separation, and negligible waste production.<sup>2</sup> Their large pore openings favor mass transport and avoid deactivation resulting from coke formation that usually takes place in microporous catalysts.<sup>3</sup> Furthermore, mesoporosity plays a significant role in catalysis involving bulky substrates and products (*e.g.* biomolecules). To date great efforts have been devoted to fabricate strong basicity on mesoporous materials. Owing to the low cost, good stability, and high synthetic controllability, mesoporous silica is the optimal choice of support among various candidates.<sup>4</sup> Hence, the generation of strong basicity on mesoporous silica has attracted massive interest ever since its discovery.

By grafting organic bases or incorporating nitrogen-containing species, some interesting basic sites can be formed on mesoporous silica.<sup>5</sup> Nonetheless, the basicity of these materials is relatively weak because of the inherent nature of basic species. To enhance the base strength, the introduction of metal oxides with strong basicity (*e.g.* K<sub>2</sub>O) was also tried; this method has been widely used for the construction of strong basicity on a range of porous supports.<sup>6</sup> The preparation includes loading of base precursors (*e.g.* the alkali metal nitrate, KNO<sub>3</sub>) and subsequent calcination to decompose the precursors to their corresponding metal oxides (*e.g.* K<sub>2</sub>O). It is worth noting that when silica is utilized as the support, quite high

temperatures are compulsory for such a well-known method. For example, the decomposition of base precursor KNO<sub>3</sub> to basic species K<sub>2</sub>O on silica only occurred at temperatures higher than 600 °C.<sup>7</sup> Apparently, energy consumption in the decomposition step is very high. Moreover, at such high temperatures the reactions of strongly basic species with siliceous supports are almost inevitable. As a result, the obtained materials only exhibit weak basicity and the mesostructure of supports is seriously damaged. Despite the efforts, the development of a facile method to create strong basicity on mesoporous silica remains a great challenge to date.

It is known that as frequently used precursors, nitrates also possess oxidizability. It is therefore possible to convert precursors to their corresponding functional oxides through the interaction with appropriate reducing agents. Herein, we report for the first time the utilization of a redox strategy to construct strong basicity on mesoporous silica, which breaks the tradition of thermally induced decomposition of base precursors. The first attempted reducing agent is methanol, whose vapor is designed to diffuse into the pores of support and interact with predispersed KNO<sub>3</sub> (Scheme 1). It is fascinating that the redox interaction makes the conversion of KNO<sub>3</sub> occur at the temperature of about 400 °C on mesoporous silica SBA-15, which is obviously lower than that of the conventional thermal decomposition of KNO<sub>3</sub> (*ca.* 600 °C). Accordingly, strong basicity is successfully generated on mesoporous silica and the ordered mesostructure is well maintained, which are



**Scheme 1** Conversion of the base precursor to strongly basic sites on mesoporous silica through (A) the conventional thermal method as well as (B) the redox strategy.

State Key Laboratory of Materials-Oriented Chemical Engineering, College of Chemistry and Chemical Engineering, Nanjing Tech University, Nanjing 210009, China. E-mail: lbsun@njtech.edu.cn; Fax: +86-25-83587191; Tel: +86-25-83587177

† Electronic supplementary information (ESI) available. See DOI: 10.1039/c5cc02502h

extremely desirable for catalysis and unlikely to be realized through traditional methods. Of course, the redox strategy is capable of saving energy since the preparation temperature is evidently declined. We also demonstrate that the resultant mesoporous solid bases exhibit excellent catalytic activity in heterogeneous transesterification reactions, which is much superior to the catalysts prepared through traditional methods as well as various typical solid strong bases.

The base precursor  $\text{KNO}_3$  was introduced into the mesoporous silica SBA-15 by impregnation (see ESI† for experimental details), and the obtained material was denoted as KS. For the conversion of  $\text{KNO}_3$  using the redox strategy, KS was heated to  $400^\circ\text{C}$  in a nitrogen flow containing the methanol vapor generated by bubbling. The resultant materials were denoted as KS-R400- $n$ , where  $n$  represents the redox time varied from 0.5 to 2 h. In a similar process, conventional thermal decomposition of  $\text{KNO}_3$  was carried out. All the conditions were identical to that in the redox process except that no methanol vapor was involved. The materials obtained from thermal treatment at  $400$  and  $600^\circ\text{C}$  were denoted as KS-T400- $n$  and KS-T600- $n$ , respectively, where  $n$  represents the treatment time.

Infrared (IR) spectroscopy was first employed to examine the conversion of  $\text{KNO}_3$  (Fig. 1A). An intense band at  $1383\text{ cm}^{-1}$  assigned to nitrate can be observed on the sample KS,<sup>8</sup> which is absent on pristine SBA-15 before the introduction of  $\text{KNO}_3$ . After thermal treatment at  $400^\circ\text{C}$  for 2 h (KS-T400-2), the band is only slightly weakened, reflecting the existence of a great deal of undecomposed  $\text{KNO}_3$ . Further enhancing the treatment temperature to  $600^\circ\text{C}$  (KS-T600-2), the intensity of the nitrate band decreases evidently. That means, supported  $\text{KNO}_3$  can be thermally decomposed at  $600^\circ\text{C}$ , whereas the mesostructure is destroyed completely as discussed later. Interestingly, the conversion of  $\text{KNO}_3$  is able to proceed smoothly at  $400^\circ\text{C}$  by the use of the redox strategy. The intensity of the nitrate band drops evidently and keeps declining with the increase of treatment time (Fig. 1A and Fig. S1, ESI†). It is

noticeable that the band is hard to identify on the KS-R400-2 sample, indicating the complete conversion of  $\text{KNO}_3$  at  $400^\circ\text{C}$  using the redox strategy. Two crystalline phases (*i.e.* orthorhombic and hexagonal phases) of  $\text{KNO}_3$  were formed on KS as displayed in the wide-angle X-ray diffraction (XRD) patterns (Fig. 1B). The diffraction lines are still visible in the KS-T400-2 sample, while they disappear in the KS-T600-2 sample that was treated thermally at  $600^\circ\text{C}$ . In the case of samples prepared using the redox strategy, the diffraction lines become weak gradually with the increase of treatment time even at  $400^\circ\text{C}$  (Fig. 1B and Fig. S2, ESI†). Also, no diffraction lines of  $\text{KNO}_3$  can be detected on the KS-R400-2 sample. The wide-angle XRD patterns thus confirm the IR results, pointing out that base precursor  $\text{KNO}_3$  can be converted efficiently through the redox strategy at the temperature as low as  $400^\circ\text{C}$ .

The structural characterization of the samples was performed by various techniques. In low-angle XRD patterns (Fig. 1C and Fig. S3 and S4, ESI†), all of the samples from redox show an intense diffraction line accompanied by two weak ones, which can be indexed as the (100), (110) and (200) reflections corresponding to the 2D hexagonal pore regularity of the  $p6mm$  space group. This suggests that the ordered mesostructure is well preserved. Due to the limited decomposition of  $\text{KNO}_3$ , the diffraction lines in low-angle XRD patterns are also observable on the KS-T400-2 sample. However, no diffraction lines can be recognized on the KS-T600-2 sample, implying the complete destruction of the mesostructure caused by the reactions between the formed strongly basic species and siliceous frameworks. Nitrogen adsorption data also give information on the structure of materials (Fig. S5–S8, ESI†). The samples from redox present isotherms of type IV with an H1 hysteresis loop, indicating that the cylindrical mesopores of SBA-15 are well maintained. Nevertheless, the KS-T600-2 sample displays neglectable  $\text{N}_2$  uptake, which gives further evidence of the collapse of the mesostructure. Transmission electron microscopy (TEM) is another useful technique to characterize the long-range channel ordering of mesoporous materials (Fig. 1D and Fig. S9, ESI†). The images of KS-R400-2 show that the periodic ordering of the mesostructure is well preserved. The results of energy dispersive X-ray spectroscopy (EDX) elemental mapping demonstrate the presence of silicon, potassium, and oxygen, and potassium is uniformly dispersed (Fig. S10, ESI†). That means, well-dispersed  $\text{K}_2\text{O}$  can be formed over the silica support. On the basis of aforementioned results, it is conclusive that the redox strategy benefits the preservation of the ordered mesostructure and that thermal treatment at  $600^\circ\text{C}$  results in the complete damage of the mesostructure although supported  $\text{KNO}_3$  can be decomposed.

The basicity of resultant materials was first characterized by the amount of basic sites (Fig. S11, ESI†). As for the samples prepared through the thermal method, the amount of basic sites is only  $0.52\text{ mmol g}^{-1}$  (KS-T400-2) and  $0.02\text{ mmol g}^{-1}$  (KS-T600-2), owing to the incomplete decomposition of  $\text{KNO}_3$  and/or the reaction of strongly basic species with siliceous support. Remarkably, for the sample after the redox treatment for 0.5 h (KS-R400-0.5), the amount of basic sites increases sharply to  $1.29\text{ mmol g}^{-1}$ . The amount of basic sites keeps increasing with the increase of treatment time and reaches  $1.87\text{ mmol g}^{-1}$  in the case of the sample treated for 2 h (KS-R400-2). Notably, this value is quite close to the theoretical value ( $1.98\text{ mmol g}^{-1}$ ), thus suggesting the nearly complete conversion of

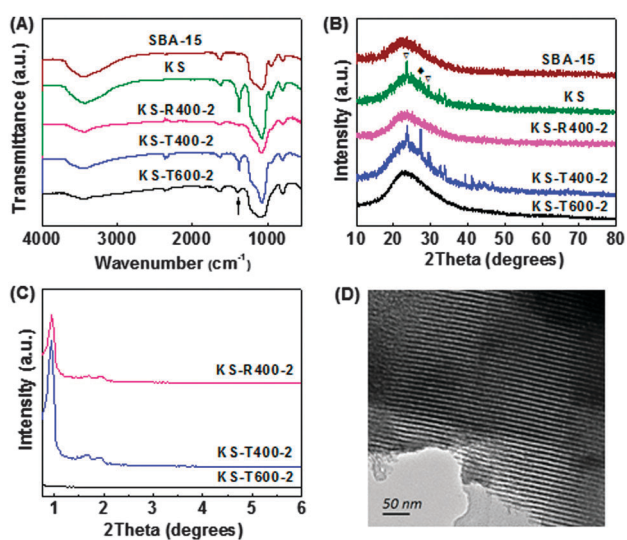


Fig. 1 (A) IR spectra, (B) wide-angle XRD patterns, and (C) low-angle XRD patterns of SBA-15 as well as KS before and after thermal or redox treatment.  $\nabla$  and  $\blacklozenge$  denote  $\text{KNO}_3$  of orthorhombic and hexagonal phases, respectively. (D) A typical TEM image of the KS-R400-2 sample.

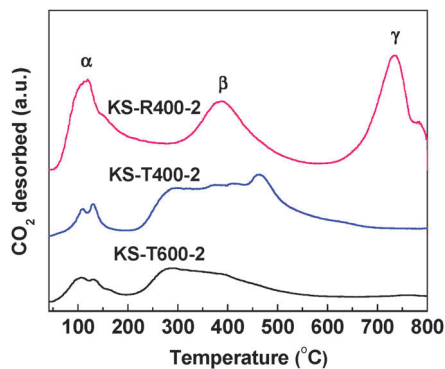


Fig. 2  $\text{CO}_2$ -TPD profiles of KS-R400-2, KS-T400-2, and KS-T600-2.

$\text{KNO}_3$  to basic sites *via* the redox strategy. Temperature programmed desorption of  $\text{CO}_2$  ( $\text{CO}_2$ -TPD) was employed to further evaluate the basicity (Fig. 2). The desorption peaks can be tentatively divided into three parts denoted as  $\alpha$ ,  $\beta$ , and  $\gamma$  at approximately 100, 350, and 700 °C, respectively, which are attributed to weak, medium, and strong basicity. Both the samples derived from thermal treatment (KS-T400-2 and KS-T600-2) give rise to desorption peaks originated from weak and medium basicity. It is noticeable that the sample prepared by the redox strategy (KS-R400-2) shows an intense peak caused by strongly basic sites in addition to weak and medium ones. Moreover, the desorption of  $\text{CO}_2$  temperature persists up to 800 °C, which is comparable to, if not higher than, some solid superbases,<sup>9</sup> thus revealing the presence of unusually strong basicity on the KS-R400-2 sample.  $\text{CO}_2$ -TPD profiles of samples derived from different redox times are presented in Fig. S12 (ESI<sup>†</sup>). With the increase of redox time, some new peaks at medium and high temperatures become visible gradually. This clearly demonstrates that the redox time affects not only the amount of basic sites but also their strength. According to these results, it is safe to say that the redox strategy is pretty efficient for the fabrication of basic sites with regard to both amount and strength.

Our materials were also utilized to catalyze the synthesis of dimethyl carbonate (DMC) *via* the transesterification of ethylene carbonate and methanol.<sup>10</sup> As a versatile green chemical, DMC has been proposed as a polar solvent, methylating and carbonylating agent, as well as a fuel additive.<sup>11</sup> Traditionally, DMC is synthesized by the use of homogeneous strong base catalysts, while increasing attention has been paid to the development of heterogeneous catalysts recently. As shown in Fig. 3, no DMC is produced at all even after the reaction for 4 h over pristine SBA-15. Under the catalysis of KS-T400-2 and KS-T600-2, the yield of DMC is 12.3% and 3.2%, respectively. It is worth noting that the samples from redox exhibit excellent catalytic performance. Even over the sample treated for only 0.5 h (KS-R400-0.5), 26.3% of DMC can be produced (Fig. S13, ESI<sup>†</sup>). With increasing treatment time, the yield of DMC continues to increase. Surprisingly, when KS-R400-2 is used as the catalyst, the yield of DMC reaches 44.3%, which is much higher than that over KS-T400-2 and KS-T600-2 despite the identical potassium content. In order to elucidate the catalytic performance of our materials deeply, some well-known solid bases were applied to make a comparison (Table S1, ESI<sup>†</sup>). Only 7.6% of DMC is yielded over the typical solid base MgO. Two zeolites with strong

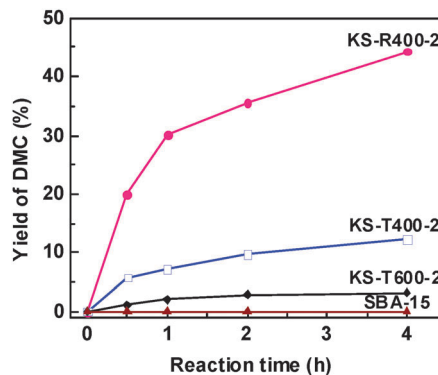
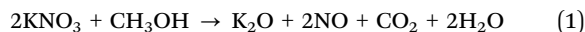


Fig. 3 The yield of DMC *via* the transesterification of ethylene carbonate and methanol under the catalysis of different samples.

basicity, namely KL and CsX, give the DMC yield of 4.0% and 6.1%, respectively. Strongly basic metal oxides were loaded on famous porous supports  $\text{Al}_2\text{O}_3$  and  $\text{ZrO}_2$ , producing solid strong bases  $\text{Li}_2\text{O}/\text{Al}_2\text{O}_3$ ,  $\text{Na}_2\text{O}/\text{Al}_2\text{O}_3$  and  $\text{CaO}/\text{ZrO}_2$ . The three catalysts give the DMC yield of 18.8%, 28.2%, and 15.1%, respectively. CaO has been regarded as a promising candidate among alkali and alkaline earth metal oxides for generation of strong basicity on mesoporous silica.<sup>9b</sup> However, over CaO/SBA-15 the yield of DMC is only 13.4%. Two mesoporous solid bases prepared using the dual coating strategy, *i.e.*  $\text{K}_2\text{O}/\text{C}/\text{SBA-15}$ <sup>9a</sup> and  $\text{K}_2\text{O}/\text{ZrO}_2/\text{SBA-15}$ ,<sup>7</sup> present 38.6% and 28.4% DMC yield, respectively. Based on these results, it is clear that the obtained materials show excellent catalytic performance, which is superior to a series of well-known solid strong bases and even superbases with various pore structures.

To investigate the pathway for the conversion of  $\text{KNO}_3$ , gaseous products formed in the process were analyzed using a mass spectrometer (MS). The signals with  $m/z$  values of 2, 18, 28, 30, and 44 were detected and can be attributed to  $\text{H}_2$ ,  $\text{H}_2\text{O}$ ,  $\text{CO}$ ,  $\text{NO}$ , and  $\text{CO}_2$ , respectively, regardless of the methods used for  $\text{KNO}_3$  conversion (Fig. 4). Two additional signals with  $m/z$  values of 31 and 32 were also monitored, and their origins are dependent on the methods. For the thermal conversion of  $\text{KNO}_3$ , the  $m/z$  signal of 32 comes from  $\text{O}_2$ . However, for the redox conversion of  $\text{KNO}_3$ , the  $m/z$  signals of 32, together with 31, should have originated from methanol. As shown in Fig. 4B, both signals (31 and 32) present the same changing trend. In terms of these MS data, the pathway for the conversion of  $\text{KNO}_3$  can be illustrated. Thermal decomposition of  $\text{KNO}_3$  on SBA-15 mainly takes place at about 600 °C, and the predominant products include  $\text{NO}$  and  $\text{O}_2$  as shown in eqn (1).



It is interesting to note that the presence of reducing agent methanol leads to a quite different pathway for the conversion of  $\text{KNO}_3$ . The conversion of  $\text{KNO}_3$  occurs at the temperature as low as 400 °C, and  $\text{NO}$ ,  $\text{CO}_2$ , and  $\text{H}_2\text{O}$  become the main gaseous products. When the temperature is higher than 500 °C, the decomposition of methanol can be observed, as the signals of  $\text{H}_2$  and  $\text{CO}$  increase sharply while the signals of methanol decrease noticeably. In this regard, the redox conversion of  $\text{KNO}_3$  on SBA-15 should be operated at temperatures lower than 500 °C. On the basis of these results, it is justified that the redox

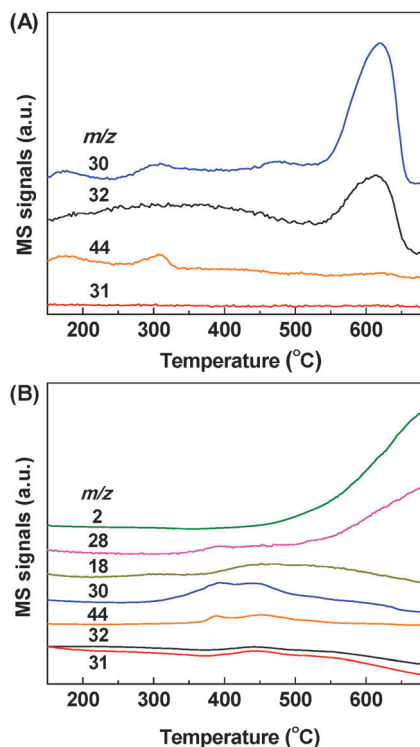


Fig. 4 MS-monitored conversion of  $\text{KNO}_3$  supported on SBA-15 through (A) the conventional thermal method and (B) the redox strategy.

strategy is able to convert base precursor  $\text{KNO}_3$  at much lower temperatures, and the conversion proceeds *via* a quite different pathway. An *in situ* IR technique was employed to further examine the redox mechanism. As presented in Fig. S14 (ESI<sup>†</sup>), the bands at 2963 and 2857  $\text{cm}^{-1}$  attributed to the C–H stretching vibration are caused by methanol adsorbed on the surface of the sample.<sup>12</sup> The bands at 3490 and 1653  $\text{cm}^{-1}$  assigned to  $\text{H}_2\text{O}$  appear and become intense gradually with the increase of time.<sup>13</sup> A similar trend is also observed on the bands of  $\text{CO}_2$  at 2370 and 2310  $\text{cm}^{-1}$ , and the intensity increases with prolonging time. Meanwhile, an opposite peak at 3745  $\text{cm}^{-1}$  assigned to the Si–OH bending vibration is detected.<sup>14</sup> That means, the Si–OH on the sample was consumed in the redox process. On the basis of these results, it is clear that  $\text{CO}_2$  and  $\text{H}_2\text{O}$  were produced from adsorbed methanol due to the redox reaction. These results are in good agreement with that from MS.

In summary, an unprecedented strategy was developed to fabricate strong basicity on mesoporous silica by using the redox interaction between a base precursor ( $\text{KNO}_3$ ) and a reducing agent (methanol). By using the redox strategy, the complete conversion of  $\text{KNO}_3$  can be achieved at much lower temperatures as compared with the conventional thermal method. Work is in progress to extend this facile redox strategy to the formation of various functional oxides from their corresponding nitrate and even acetate precursors, especially aiming to introduce the functionality that is impossible or difficult to achieve through conventional thermal methods.

This work was supported by the Distinguished Youth Foundation of Jiangsu Province (BK20130045), the Fok Ying-Tong Education Foundation (141069), the National High Technology Research and Development Program of China (863 Program, 2013AA032003), the National Basic Research Program of China (973 Program, 2013CB733504), and the Project of Priority Academic Program Development of Jiangsu Higher Education Institutions.

## Notes and references

- (a) S. Pradhan, J. K. Bartley, D. Bethell, A. F. Carley, M. Conte, S. Golunski, M. P. House, R. L. Jenkins, R. Lloyd and G. J. Hutchings, *Nat. Chem.*, 2012, 4, 134; (b) F. A. Westerhaus, R. V. Jagadeesh, G. Wienhofer, M. M. Pohl, J. Radnik, A. E. Surkus, J. Rabeah, K. Junge, H. Junge, M. Nielsen, A. Bruckner and M. Beller, *Nat. Chem.*, 2013, 5, 537; (c) M. Cargnello, V. V. T. Doan-Nguyen, T. R. Gordon, R. E. Diaz, E. A. Stach, R. J. Gorte, P. Fornasiero and C. B. Murray, *Science*, 2013, 341, 771.
- (a) G. Busca, *Chem. Rev.*, 2010, 110, 2217; (b) P. D. Raytchev, A. Bendjeriou, J. P. Dutasta, A. Martinez and V. Dufaud, *Adv. Synth. Catal.*, 2011, 353, 2067; (c) P. Puthiaraj and K. Pitchumani, *Chem. – Eur. J.*, 2014, 20, 8761.
- (a) X. Jin, V. V. Balasubramanian, S. T. Selvan, D. P. Sawant, M. A. Chari, G. Q. Lu and A. Vinu, *Angew. Chem., Int. Ed.*, 2009, 48, 7884; (b) A. Corma, *Chem. Rev.*, 1997, 97, 2373; (c) G. D. Yadav and J. Y. Salunke, *Catal. Today*, 2013, 207, 180.
- (a) Y. H. Deng, J. Wei, Z. K. Sun and D. Y. Zhao, *Chem. Soc. Rev.*, 2013, 42, 4054; (b) S. S. Kim, W. Z. Zhang and T. J. Pinnavaia, *Science*, 1998, 282, 1302; (c) W. J. Jiang, Y. Yin, X. Q. Liu, X. Q. Yin, Y. Q. Shi and L. B. Sun, *J. Am. Chem. Soc.*, 2013, 135, 8137; (d) L.-B. Sun, J.-R. Li, W. Lu, Z.-Y. Gu, Z. Luo and H.-C. Zhou, *J. Am. Chem. Soc.*, 2012, 134, 15923.
- (a) S. Y. Chen, C. Y. Huang, T. Yokoi, C. Y. Tang, S. J. Huang, J. J. Lee, J. C. C. Chan, T. Tatsumi and S. Cheng, *J. Mater. Chem.*, 2012, 22, 2233; (b) L. B. Sun, J. Shen, F. Lu, X. D. Liu, L. Zhu and X. Q. Liu, *Chem. Commun.*, 2014, 50, 11299; (c) Y. D. Xia and R. Mokaya, *Angew. Chem., Int. Ed.*, 2003, 42, 2639; (d) K. Sugino, N. Oya, N. Yoshie and M. Ogura, *J. Am. Chem. Soc.*, 2011, 133, 20030.
- (a) X. Y. Liu, L. B. Sun, F. Lu, X. D. Liu and X. Q. Liu, *Chem. Commun.*, 2013, 49, 8087; (b) R. Sundararaman and C. Song, *Appl. Catal., B*, 2014, 148, 80; (c) L. B. Sun, J. Yang, J. H. Kou, F. N. Gu, Y. Chun, Y. Wang, J. H. Zhu and Z. G. Zou, *Angew. Chem., Int. Ed.*, 2008, 47, 3418.
- X. Y. Liu, L. B. Sun, F. Lu, T. T. Li and X. Q. Liu, *J. Mater. Chem. A*, 2013, 1, 1623.
- L. B. Sun, F. N. Gu, Y. Chun, J. Yang, Y. Wang and J. H. Zhu, *J. Phys. Chem. C*, 2008, 112, 4978.
- (a) X.-Y. Liu, L.-B. Sun, X.-D. Liu, A.-G. Li, F. Lu and X.-Q. Liu, *ACS Appl. Mater. Interfaces*, 2013, 5, 9823; (b) L. B. Sun, J. H. Kou, Y. Chun, J. Yang, F. N. Gu, Y. Wang, J. H. Zhu and Z. G. Zou, *Inorg. Chem.*, 2008, 47, 4199; (c) L. B. Sun, Y. H. Sun, X. D. Liu, L. Zhu and X. Q. Liu, *Curr. Org. Chem.*, 2014, 18, 1296.
- (a) M. Honda, A. Suzuki, B. Noorjahan, K.-i. Fujimoto, K. Suzuki and K. Tomishige, *Chem. Commun.*, 2009, 4596; (b) F. J. Liu, W. Li, Q. Sun, L. F. Zhu, X. J. Meng, Y. H. Guo and F. S. Xiao, *ChemSusChem*, 2011, 4, 1059; (c) G. Stoica, S. Abello and J. Perez-Ramirez, *ChemSusChem*, 2009, 2, 301; (d) A. F. Lee, J. A. Bennett, J. C. Manayil and K. Wilson, *Chem. Soc. Rev.*, 2014, 43, 7887.
- (a) T. T. Li, L. B. Sun, X. Y. Liu, Y. H. Sun, X. L. Song and X. Q. Liu, *Chem. Commun.*, 2012, 48, 6423; (b) Z.-Z. Yang, Y.-N. Zhao, L.-N. He, J. Gao and Z.-S. Yin, *Green Chem.*, 2012, 14, 519.
- R. Ladera, E. Finocchio, S. Rojas, J. Fierro and M. Ojeda, *Catal. Today*, 2012, 192, 136.
- M. F. Baruch, J. Pander, J. L. White and A. B. Bocarsly, *ACS Catal.*, 2015, 5, 3148.
- A. Bendjeriou-Sedjerari, J. D. Pelletier, E. Abou-Hamad, L. Emsley and J.-M. Basset, *Chem. Commun.*, 2012, 48, 3067.